Rotational Relaxation in a Nondipolar Supercritical Fluid: Toluene in CO_2†

Ali Siavosh-Haghighi and John E. Adams*

Department of Chemistry, University of Missouri-Columbia, Columbia, Missouri 65211-7600

Received: October 16, 2000; In Final Form: January 17, 2001

Studies of rotational relaxation dynamics provide particular insight into local solution structures and consequently into the interactions between species in a solution. We report here the results of molecular dynamics simulations describing a neat CO_2 supercritical fluid and an infinitely dilute solution of toluene in supercritical CO_2. Over a period of 0.1−0.2 ps, the rotation of the near-critical solvent molecules is relatively unhindered, becoming purely diffusive only on a time scale that is long compared with the decay of the orientational correlations. As expected, the rotational relaxation rate of a toluene molecule is found to increase with increasing solvent density, although the simulation results imply some anomalous behavior near the critical point that may be associated with the appearance of long-range spatial correlations. We also show that a system consisting of a nonpolar toluene analogue experiences an isotropic rotational friction environment, unlike the anisotropic environment in which a real toluene molecule is found when dissolved in supercritical CO_2.

I. Introduction

Because their densities may be varied continuously over a wide range, supercritical fluids (SCFs) afford an unparalleled medium for the study of solvation phenomena. Much attention recently has focused on a particularly intriguing aspect of these systems, the appearance of density inhomogeneities in the near-critical regime,[1−13] but SCFs also have proven the solvents of choice in more general investigations of fluid dynamics.[14−16] Our emphasis here is on the characterization of solute rotational dynamics, which is profoundly affected by local solute−solvent interactions. Those interactions yield, in the language suggested by the casting of the problem in terms of an appropriate generalized Langevin equation,[17] a local-density-dependent rotational friction.[15,18−20] Both Maroncelli[21−23] and Waldeck,[24,25] and their respective co-workers, have investigated the contributions to this friction, which can be fundamentally "mechanical" in character (i.e., deriving from the short-range forces conventionally characterized in terms of Lennard-Jones interactions) or "dielectric" (a consequence of permanent molecular electrical moments). Although it would be convenient to view these two contributions as being independent and hence separable,[26] Maroncelli has shown in very recent work[22] that any attempted separation is intrinsically flawed. Even short-range electrostatic effects alter the local density profile and thus produce a nonnegligible change in the friction deriving from what otherwise would be viewed as purely mechanical contributions.

For practical reasons most studies of solute rotational relaxation have utilized rather large chromophore molecules having substantial dipole moments and, quite often, dipolar solvents.[24−28] However, by selecting toluene and CO_2, respectively, as our solute and solvent for study, we choose a quite different sort of system, one not dominated by dipole−dipole interactions. That is not to say that no dielectric frictional effects are expected here, since the small dipole moment of the aromatic molecule (experimentally 0.36 D,[29] 0.24 D in the potential model used herein[30]) will interact with the large quadrupole moment[31] of CO_2 (-1.4×10^{-39} C·m^2), but it is not clear just how great an effect these shorter-range (as compared with dipole−dipole) interactions will have on the rotational dynamics. Stokes shift measurements by Maroncelli and co-workers[16] of coumarin 153 in a variety of solvents have suggested that solvation in nondipolar solvents, while qualitatively very similar to what is seen in dipolar solvents, is not quantitatively modeled by theories parametrized by the solvent's dielectric constant, i.e., by standard continuum dielectric models.[32] Very recent work by Khajehpour and Kauffman[33] also has indicated that quadrupolar fluids can have a considerable effect on the observed emission spectra of solutes and that in SCF CO_2 the quadrupole moment of the solvent may be largely responsible for the commonly observed local density enhancements in the near-critical regime.

If one follows the rotation of an equilibrated solute molecule beginning at some arbitrary zero of time, one expects that there will be an interval, possibly very short, during which the solute rotates freely within its solvent cage.[34] Rotational relaxation dynamics in this regime is essentially inertial in character. On a much longer time scale, however, the actual dynamics is quite different and is more likely to be approximated reasonably well by a Debye model,[35] whereby rotational relaxation results from a myriad of uncorrelated collisions with solvent molecules. The time scale associated with the transition between these inertial and diffusive regimes depends on the local solvation environment, which in turn reflects the solute−solvent interactions and the solvent density. But also reflected is the geometry of the solute molecule—a large solute necessarily collides almost immediately with solvent species upon undergoing even a very small angular displacement. For that reason we focus on a small solute molecule (toluene), hypothesizing that the inertial dynamical regime persists long enough for it to be readily probed, especially at subcritical densities.

Of course, understanding the dynamics of a single toluene molecule dissolved in SCF CO_2 becomes easier if one already has a sense of the dynamics of the solvent molecules themselves.

† Part of the special issue "William H. Miller Festschrift".

* To whom correspondence should be addressed. E-mail: AdamsJE@missouri.edu.

10.1021/jp003787o CCC: $20.00
Published on Web 03/01/2001

We therefore began our study by briefly investigating the neat fluid. (A more extensive study of CO_2 is being carried out, however, and will be the subject of another publication.[36]) Relatively few inquiries into density-dependent rotational relaxation in pure SCFs have appeared, at least in comparison with similar studies on "ordinary" liquids. A good example of such work, though, is the experimental and theoretical work on CHF_3 reported by Okazaki et al.,[37] who observed an onset of liquidlike diffusional relaxation near the critical density. They also found (at least qualitatively) much the same sort of density inhomogeneities in the near-critical regime that Goodyear, Maddox, and Tucker[10] characterized in their two-dimensional model studies. CO_2 also has been examined by Versmold,[38] who carried out depolarized Rayleigh scattering experiments at state points significantly removed from the critical density. Although the results obtained in the subsequent simulation by Böhm, et al.,[39] are in reasonably good agreement with Versmold's experimental data,[38] the significance of this agreement is unclear, since the phase diagram corresponding to their potential model is unknown. (This agreement also is in contrast to that afforded by the work of Singer et al.,[40,41] who employed a CO_2 potential energy description that predicts a zero quadrupole moment.) Thus, there remains cause for examining the density-dependent dynamical properties of SCF CO_2 using a potential function that correctly predicts the position of the critical point.

II. Theoretical and Computational Background

A. Correlation Functions. Time correlation functions provide a convenient and powerful formalism for encapsulating the relaxation dynamics of a molecular system. Of particular interest in the case of rotational relaxation are orientational correlation functions[18] of the form

$$C_l(t) = \langle P_l(\mathbf{u}(0)\cdot\mathbf{u}(t))\rangle$$

where $\mathbf{u}$ is a unit vector directed along one of the principal axes of the molecule, and $P_l(z)$ is an lth order Legendre polynomial. The choice of l here depends on the particular process being modeled; for example, $l = 1$ for infrared absorption and $l = 2$ for Raman scattering and fluorescence depolarization. For a molecule having a permanent dipole moment, it is usually appropriate that $\mathbf{u}$ be taken in the direction of the permanent dipole. Integration of $C_l(t)$ then yields a corresponding rotational correlation time,

$$\tau_R^{(l)} = \int_0^\infty C_l(t)\, dt$$

For a linear molecule in the Debye (Brownian particle) limit,[35] these orientational correlation functions are known to reduce to a particularly simple exponential form,[18]

$$C_l(t) = e^{-l(l+1)D_R t} \qquad (2.1)$$

where D_R is the rotational diffusion constant.

Alternatively, one may characterize rotational relaxation by calculating an angular velocity correlation function of the form

$$C_{\omega_i}(t) = \frac{\langle \omega_i(0)\, \omega_i(t)\rangle}{\langle \omega_i(0)^2\rangle} \qquad (2.2)$$

where the rotation is about a principal axis i of the molecule. For a linear molecule, molecular rotation is isotropic, and thus $C_{\omega_i}(t)$ is the same for rotation about any axis perpendicular to the molecular axis (and will be denoted merely as $C_\omega(t)$).

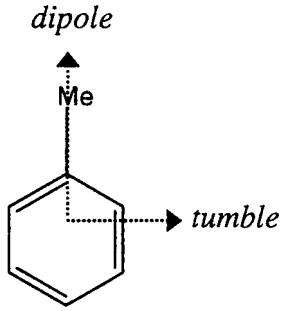

Figure 1. Structure of toluene showing the principal rotational axes, labeled as described in the text. The third rotation axis, about which the molecule undergoes planar rotation, lies normal to the plane of the aromatic ring.

Rotation of a molecule like toluene, however, is characterized by three distinct correlation functions, corresponding to (1) rotation in the plane of the aromatic ring, (2) end-over-end tumbling, and (3) rotation about the dipole axis, which lies in the direction of the methyl group (Figure 1).

A particular practical advantage to the use of angular velocity correlation functions is that they generally decay on a faster time scale than do the analogous orientational correlation functions. Furthermore, they provide direct access to axis-specific rotational diffusion constants, which are obtained straightforwardly via integration.[18,24]

$$D_i = \int_0^\infty \langle \omega_i(0)\omega_i(t)\rangle\, dt$$

$$= \langle \omega_i(0)^2\rangle \int_0^\infty C_{\omega_i}(t)\, dt$$

where $\langle \omega_i(0)^2\rangle = k_B T/I_i$, I_i being the moment of inertia about the ith principal axis. They also lead directly to values of the total (zero-frequency) rotational friction coefficient ζ_{R_i}, which are given (in the limit of diffusive dynamics) by $\zeta_{R_i} = k_B T/D_i$, and to characteristic relaxation times,

$$\tau_R^{(\omega_i)} = \int_0^\infty C_{\omega_i}(t)\, dt$$

To describe the interactions between CO_2 molecules, we have adopted the EPM2 model devised by Harris and Yung,[42] an all-atom, pairwise-additive potential consisting of Lennard-Jones and Coulomb terms. Although a number of CO_2 potentials are readily available in the literature,[43] the EPM2 model is particularly appropriate for the present work, because its parameters have been scaled such that the critical point and liquid−vapor coexistence curve are reproduced. Many will recognize this basic functional form as being that of the all-atom OPLS potential suggested by Jorgensen et al.[44,45] The most reasonable choice for a toluene potential parametrization is thus Jorgensen's,[30] which in this case includes the useful simplification of replacing the methyl group with a single spherical interaction site. The Lennard-Jones parameters for the toluene−CO_2 interactions are subsequently obtained using the conventional combining rules of the OPLS model, namely $\epsilon_{ij} = \sqrt{(\epsilon_i \epsilon_j)}$ and $\sigma_{ij} = \sqrt{(\sigma_i \sigma_j)}$. All the molecules in these studies are assumed rigid, fixed at their equilibrium geometries.

B. Simulations. The molecular dynamics (MD) simulations on which this work is based are reasonably standard, having been performed using the *Moldy* code,[46] which implements a modified Beeman integration algorithm[47] (accurate to order δt^4 in the coordinates and δt^3 in the velocities) to solve the center-of-mass and quaternion dynamical equations. In all cases reported here we began with 1024 CO_2 molecules (and, for the

solvation studies, a single toluene molecule) in a (periodically replicated) cubic box, the edge length of which is chosen so as to yield the desired solvent density. The long-range Coulomb forces are calculated using Ewald sums with conducting boundary conditions.[48] Although Harris and Yung[42] used a reaction field method for computing the contribution of these forces, we have chosen to follow the lead of workers such as Ladanyi[49] and Maroncelli,[3] who also have opted for calculating Ewald sums, either directly or with a spherical truncation. Furthermore, we have made the conventional assumption that we are working in the infinite dilution limit, that the presence of a toluene solute molecule does not perturb significantly the position of the critical point of CO_2.

We also have begun exploring the role of electrostatic effects on rotational relaxation by conducting a few simulations in which the Coulomb terms are omitted from some or all of the potential functions. Any comparison between these results and those deriving from simulations performed using the full potential function is imperfect, in a sense, because we have not compensated for the loss of the electrostatic contribution to the binding energies by adjusting the Lennard-Jones well-depth parameters. Nevertheless, we should be able to estimate the magnitude of the net contribution of the dielectric environment to the dynamics in this way. Of course, rescaling Lennard-Jones potentials in order to preserve net binding energies can be fraught with difficulties as well; a simple rescaling of the solvent potential certainly need not yield the same system critical parameters due to the differences in the length scales over which the Lennard-Jones and Coulomb potentials act.

Prior to generating the trajectories used in calculating the correlation functions, we equilibrated our systems by performing 300 ps *NVT* simulations ($\delta t = 0.005$ ps), the temperature being set to $T^* = T/T_c = 1.01$ and maintained via periodic rescalings of the velocities. (The critical temperature[50] T_c is 304.2 K, so T^* corresponds to 307 K. This temperature was used in all the simulations described in this work.) Since the various popular thermostating algorithms[48] all produce an unknown effect on the dynamics of individual molecules, the simulations for analysis were all performed at constant energy. Specifically, 10 segments of 10 ps each were generated using a time step of 0.002 ps, with a rescaling of the velocities being implemented prior to the beginning of each new segment to compensate for integrator drift over the previous segment and (when necessary) to reequilibrate the toluene molecule. (The energy fluctuations of the single toluene molecule are necessarily far greater than are those of the aggregate solvent.) Correlation functions were then calculated over each of these 10 segments from molecular positions and velocities (extracted from the quaternions and the quaternion velocities) stored at 0.04 ps intervals (i.e., every 20 simulation time steps) and were averaged to produce the final reported results.

III. Neat CO_2

To characterize the structure of an equilibrated CO_2 fluid, we computed radial distribution functions (RDFs) at a variety of fluid densities. (These RDFs, calculated on the basis of the final 10000 steps of the *NVT* simulation, reflect the distribution of molecular centers of mass, i.e., of the carbon atoms.) Representative results from those calculations are displayed in Figure 2 to a distance of 1.5 nm. The obvious change obtained upon increasing the density is the appearance of a clear second solvation shell as one reaches the critical density, and (although it is not obvious from the plots presented) the hint of a third shell appearing at about the same density. One also finds that

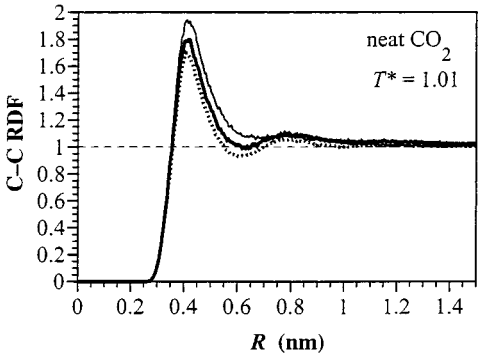

Figure 2. Radial distribution functions for supercritical CO_2 at 307 K. The thin solid line corresponds to a density of 0.200 g/cm^3 ($\rho^* = 0.427$); the thick solid line corresponds to a density of 0.468 g/cm^3 ($\rho^* = 1.00$); the dotted line corresponds to a density of 0.600 g/cm^3 ($\rho^* = 1.28$).

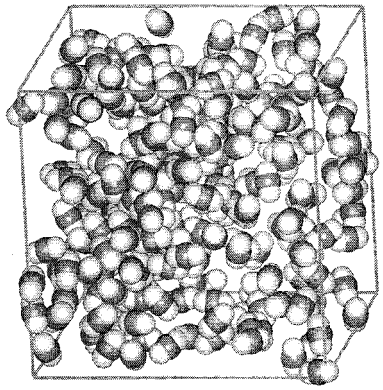

Figure 3. Snapshot of supercritical CO_2 from a simulation at 307 K and a density equal to the critical density. For purposes of clarity, only 256 molecules were included in this simulation.

the RDF remains distinctly greater than unity to longer distances at the critical density than it does at the other two densities shown, a result that is consistent with the presence of macroscopic correlations in an SCF in the immediate vicinity of its critical point. These RDFs do not provide, though, inasmuch as they are highly averaged (both in time (25 ps) and over all 1024 CO_2 molecules), a sense of the instantaneous fluid structure. A single snapshot (orthographic projection) of that structure is given in Figure 3 for a slightly simpler system containing only 256 molecules at the critical density. There is no qualitative difference between the results of Figure 3 and those obtained in a simulation with 1024 molecules, but it is more difficult to discern the structure in the larger system when the three-dimensional cell is projected onto two dimensions.) Note, in particular, the presence of open channels that extend entirely through the cell. Clearly, one finds in these simulations the same sort of density inhomogeneities reported by Tucker and co-workers[10] in their two-dimensional SCF work and depicted by Okazaki et al.[37] for three-dimensional CF_3H. This finding suggests that our implementation of the Harris and Yung potential[42] indeed yields reasonable values for the critical parameters and that our chosen temperature places us in the near-critical regime.

We turn now to the calculated correlation functions for neat CO_2, which are displayed in Figure 4, for a system at the critical density. (Note also the corresponding rotational relaxation parameters given in Table 1.) Comparing the two orientational functions, we find that $C_2(t)$ decays on a shorter time scale than does $C_1(t)$, just as one would expect on the basis of the predicted long-time diffusive behavior captured in eq 2.1. That diffusive

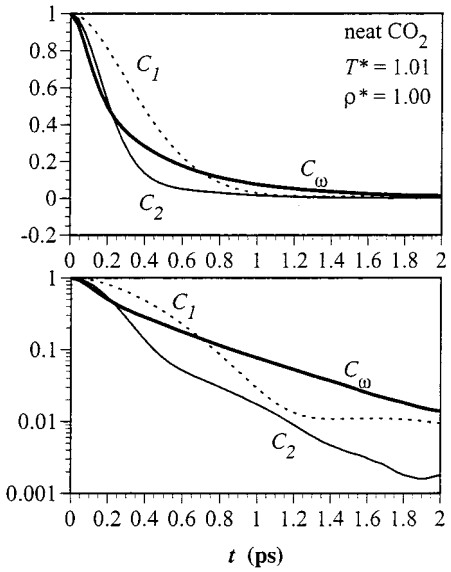

Figure 4. Time correlation functions for near-critical CO_2 as defined by eqs 2.1 and 2.2. The upper and lower panels differ only in the scale used (linear in the upper and logarithmic in the lower) in the plotting the ordinate.

TABLE 1: Calculated Rotational Parameters, $T^* = 1.01$

	$\rho^* =$ 0.427	$\rho^* =$ 1.00	$\rho^* =$ 1.28	$\rho^* =$ 1.00 ($\mu_{Tol} = 0$)
		CO_2		
$\tau_R^{(1)}$ (ps)		0.44		
$\tau_R^{(2)}$ (ps)		0.26		
$\tau_R^{(\omega)}$ (ps)		0.36		
D_R (ps^{-1})		2.2		
ζ_R ($\times 10^{-32}$ J·s)[a]		0.19		
		Toluene−CO_2		
		Planar		
$\tau_R^{(\omega)}$ (ps)	0.58	0.33	0.46	0.34
D_R (ps^{-1})	0.43	0.23	0.40	0.25
ζ_R ($\times 10^{-32}$ J·s)	0.99	1.9	1.06	1.7
		Tumble		
$\tau_R^{(\omega)}$ (ps)	0.080	0.17	0.089	0.20
D_R (ps^{-1})	0.088	0.22	0.14	0.23
ζ_R ($\times 10^{-32}$ J·s)	4.8	1.9	3.0	1.8
		Dipole		
$\tau_R^{(\omega)}$ (ps)	0.20	0.18	0.14	0.076
D_R (ps^{-1})	0.57	0.53	0.42	0.22
ζ_R ($\times 10^{-32}$ J·s)	0.74	0.80	1.0	1.9

[a] For reference, a friction coefficient is given even though the dynamics is not necessarily diffusive.

regime is not achieved in the 2 ps time interval depicted, however. Even though both C_1 and C_2 are effectively zero after 1 ps, C_ω tails away more slowly. Indeed, only for $t > 2$ ps has the angular velocity of CO_2 relaxed entirely. It is therefore not surprising that the logarithmic plots of C_1 and C_2 shown in the lower panel of Figure 3 are not the straight lines with slopes in the ratio 1:3 that would be found if eq 2.1 were applied. (The shapes of these later curves at longer times, when $C_l(t) < 0.01$, are relatively uncertain, but it nonetheless is clear that the behavior predicted by a purely diffusive model does *not* obtain here at times shorter than 2 ps. Subsequent work[36] has revealed that $C_\omega(t)$ exibits faster decay than $C_l(t)$, $l = 1$ or 2, only when $\rho_{CO_2} > 0.6$ g·cm^{-3}. At these higher densities, diffusive dynamics is indicated after an initial 0.1−0.3 ps period.)

At first glance all of the correlation functions appear to exhibit a quadratic time dependence at very short times (<0.1−0.2 ps). If the rotational dynamics of CO_2 is essentially ballistic on that time scale, then the data should be consistent with the short-time expansions of C_l and C_ω appropriate to (nearly) free-rotor dynamics,[18] namely

$$C_l(t) = 1 - \frac{1}{2} l(l+1)\frac{k_B T}{I} t^2$$

$$C_\omega(t) = 1 - \frac{1}{2}\frac{\langle \mathbf{N}(0)^2 \rangle}{2Ik_B T} t^2 = 1 - \frac{\Omega_0^{\,2}}{2} t^2 \qquad (3.1)$$

where $\mathbf{N}(0)$ is the torque at time zero and Ω_0 plays the role of an average frequency of collisions that "scramble" the angular velocity. In the present case for CO_2, the coefficient multiplying t^2 in eq 3.1 is found to be $3.02l(l+1)$ ps^{-2} (i.e., 6.04 ps^{-2} when $l = 1$ and 18.1 ps^{-2} when $l = 2$). If we fit the $C_1(t)$ data shown to this quadratic form, in the limit $t \rightarrow 0$ we obtain a value of 6.3 ps^{-2} for this coefficient, which is in good agreement with the theoretical value. (A direct fit of a Gaussian to this same data yields the limiting value 6.2 ps^{-2}.) The same fitting procedure when applied to the C_ω data yields $\Omega_0 = 9.2$ ps^{-1}, which appears to be an entirely reasonable result given that in the lower panel of Figure 3, ln C_ω exhibits an inflection point in the interval $t = 0.1-0.2$ ps, and the curve is linear after about $t = 0.8$ ps.

In the above discussion when we refer to parameters obtained in the limit $t \rightarrow 0$, we mean values that are approached as we use successively fewer points in the fitting procedure. (The final limiting value is then obtained by extrapolation.) Since for both $C_1(t)$ and $C_\omega(t)$, the limiting values represent upper bounds, it appears that even on this short time scale, the rotational motion of CO_2 is not strictly free, but rather it is retarded as a result of intermolecular interactions.

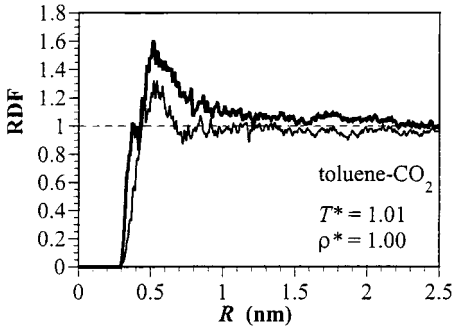

Figure 5. Radial distribution function corresponding to the disposition of the centers of mass of CO_2 solvent molecules about the center of mass of the single toluene solute molecule. The heavy line is found using the full potential energy function, while the thin line is obtained when partial charges on all the atoms in the toluene molecule are set to zero. The data shown have been smoothed somewhat according to the procedure cited in the text.

IV. Toluene−CO_2

We begin the discussion of the toluene−CO_2 results by giving the RDF for the solution at its critical density (Figure 5; R here is the distance between the toluene and CO_2 centers of mass). Because there is only one toluene molecule included in this simulation, additional time steps (a total of 50 000) must be included in the averaging to obtain noise levels more comparable with those obtained in the neat CO_2 simulations. Further smoothing has been accomplished by application of the simple algorithm detailed by Allen and Tildesley.[48] The first-shell peak seen in the RDF has two components, a broad main peak between 0.4 and 0.7 nm and a second weaker feature that appears as a distinct shoulder on the main peak just below 0.4 nm. Results from studies of benzene−CO_2 clusters[51] suggest

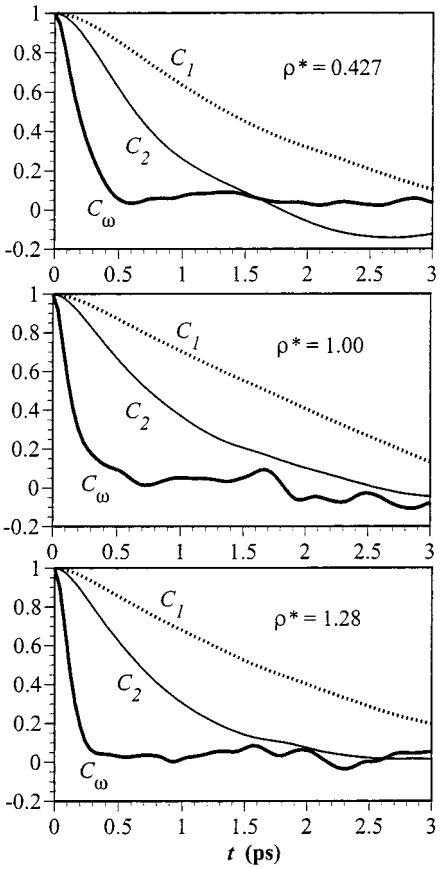

Figure 6. Time correlation functions for the rotation of toluene in supercritical CO_2 at three different densities. The temperature in all cases is 307 K.

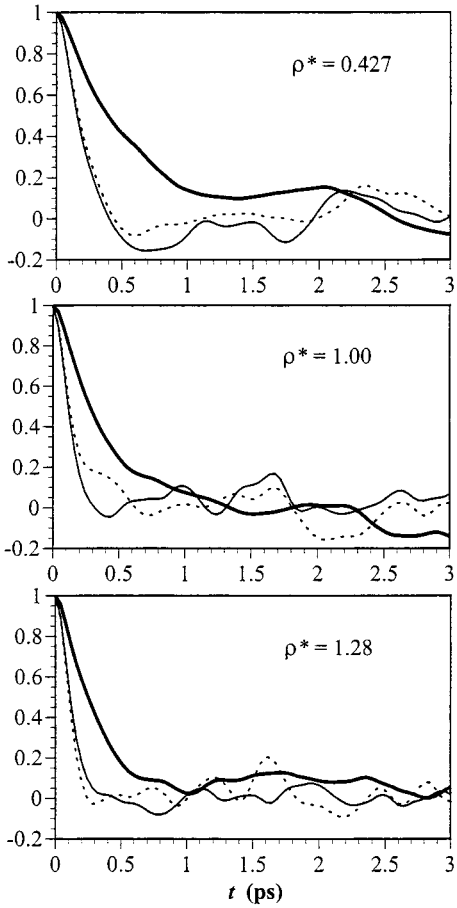

Figure 7. Angular velocity correlation functions for rotation of toluene about its three principal axes. The heavy line corresponds to rotation about the axis perpendicular to the aromatic ring; the thin line corresponds to end-over-end tumbling of the molecule about an axis lying in the plane of the aromatic ring and perpendicular to the direction of the dipole moment; the dashed line corresponds to rotation about the axis containing the molecular dipole moment vector.

that this shoulder derives from CO_2 molecules centered above and below the aromatic ring (the lowest energy binding sites reported by Nowak et al.[51] lie at a distance of 0.33 nm), while the main peak reflects a broad distribution of solvent molecules that are either displaced from the centered positions on either face of the ring or are peripheral to the ring.

The calculated correlation functions for this system at three different densities are presented in Figure 6. As the density is increased, one finds as expected that the rate at which the angular velocity relaxes increases, while little change (especially in the short-time behavior of $C_2(t)$) is found in the orientational relaxation. (Of course, one should note that the orientational relaxation does not reflect rotational motion about the axis parallel to the dipole moment of toluene, but only those rotations that reorient that dipole direction.) In the case of the solution at the critical density ($\rho^* = 1.00$), the decay of $C_1(t)$ is nearly linear over the interval $t = 1-3$ ps, while at the highest density shown, its decay is not complete until about 6 ps. One also finds a complicated oscillatory structure appearing in the angular velocity time correlation function after its initial (rapid) decay. Certainly, noise in the calculations makes attributing any physical significance to this structure problematic. But even so, the analysis would be complicated by the fact that rotation of a toluene molecule is by no means isotropic. ($C_\omega(t)$ given here is obtained from eq 2.2 by substituting the full angular momentum vector $\omega(t)$ for its component about a particular axis.) It is also worth noting that energy transfer between the single solute molecule and the solvent bath may significantly perturb the energy of the solute molecule over the time scale of a simulation. In the case of the pure solvent, even though energy transfer between molecules can impact the rotational behavior of those individual molecules, it has little impact on the calculated correlation functions due to the averaging over the large number of solvent species.

In an attempt to clarify the rotational dynamics of the solute, we have calculated angular velocity correlation functions for rotations about the individual principal axes of toluene (see Figure 1), the results of those calculations being shown in Figure 7. The heavy lines in these plots relate to rotation about the axis perpendicular to the plane of the aromatic ring; i.e., the rotational motion is strictly in the plane of the molecule. This motion is also associated with the largest moment of inertia, so the rotation about this axis is inherently slower than the other rotations. The slower decay of this correlation function is in part a consequence of the slower rotation, but it also reflects the fact that, particularly at lower densities, the CO_2 molecules prefer to aggregate above and below the ring rather than peripherally in the plane of the ring. Thus, planar rotation, which is sensitive only to these peripheral solvent molecules, is relatively unhindered in comparison with out-of-plane motions. The other two rotations, end-over-end tumbling of the methyl group (the thin solid line) and rotation about the dipole axis (the dashed line), decay on very similar time scales, at least initially. Both motions are sensitive to the presence of the CO_2 molecules in their preferred interaction sites (above and below the ring), although the tumbling motion will be influenced to a greater extent by local interactions in the vicinity of the methyl group, where the dipole−quadrupole forces are strongest. Although the statistical noise in the simulations precludes a

quantitative analysis of the dynamics at longer times, it is interesting to note that all the frequencies of the oscillations in the $C_{\omega_i}(t)$ increase as the density of the solvent increases, while the amplitudes of these oscillatory components diminish with increasing density.

The rotational parameters characterizing the correlation functions of Figure 7 are summarized in Table 1. Since integration of the oscillatory angular velocity correlation functions is problematic in any case and is especially questionable for results that are noisy at longer times, we have adopted the strategy implemented by Kurnikova et al.[24] and have fit our numerical functions to the form $y = a_1 \exp(-a_2t^2) + a_3 \exp(-a_4t) \cos(a_5t + a_6)$. Note that this form has the correct long-time behavior (decay to zero) as well as an oscillatory factor, and it may be integrated analytically. Our fits to this function emphasize the short-time data ($t < 2.5$ ps), thus minimizing any contribution from artificial oscillations resulting from incomplete averaging at longer times.

The values pertaining to rotation about the dipole axis are the most easily interpreted, so we begin there. This is the fastest rotational motion (smallest moment of inertia), thus at low densities it is characterized by the largest diffusion constant and the smallest friction coefficient. At this density, we expect that the principal toluene−solvent interaction will be with CO_2 molecules lying above and below the aromatic ring and that these molecules are most likely to be oriented in the same direction as the toluene's dipole, since that orientation places a negatively charged oxygen atom in the direction of the relatively positive methyl group. Thus, when the toluene molecule rotates about its long (dipole) axis, it can undergo a relatively large angular displacement before suffering a repulsive interaction with a solvent molecule. This dynamical behavior is only weakly density dependent due to the strongly favored interaction geometry assumed by the solvent molecules.

The end-over-end tumbling motion is the next fastest, but we find that at both the lowest and highest densities, it is associated with the most rapid rotational relaxation, smallest diffusion constants, and the largest friction coefficients. This strongly hindered rotation derives in part from interactions with the same CO_2 molecules that ultimately retard the rotation about the dipole axis, but one also must consider interactions between solvent molecules and the partially charged methyl group that contribute to the friction. Curiously, though, at the critical density tumbling appears to be less hindered, although it is also at this density that we have found it most difficult to achieve a good fit of the calculated correlation function to the form indicated above. Nonetheless, the long-range ordering of the solvent in the immediate vicinity of its critical point necessarily leads to a competition between the toluene−solvent interactions and the solvent−solvent interactions, and this competition may be inducing a structural change that leads to a net reduction in the friction felt by the methyl group as it moves through the fluid. (A small change in the positions of a few solvent molecules would be sufficient to produce the observed reduction in the friction. We will return to this point briefly in the discussion of our final model system.) At the higher system density, one then finds an increase in local density that leaves the motion once again strongly hindered.

A different behavior is seen for rotation of toluene in the plane of its ring. This is the slowest rotational degree of freedom of the molecule, but the few peripheral CO_2 molecules are not particularly effective at hindering planar rotation. As the density is increased to the critical density, solvent molecules are more likely to populate the generally repulsive peripheral sites, and

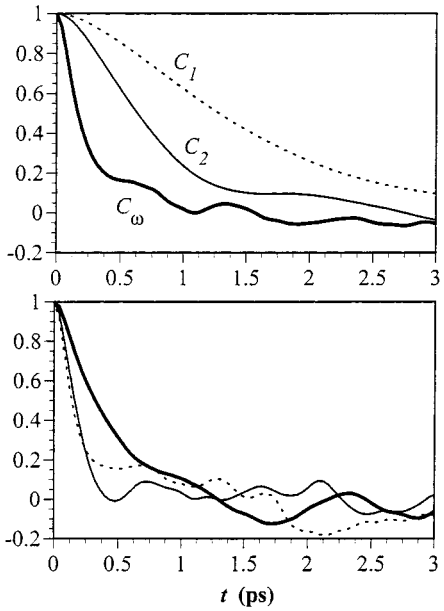

Figure 8. Upper panel: time correlation functions for a model system identical to toluene-CO_2 except that the partial charges on the toluene analogue have been set to zero. Lower panel: angular velocity correlation functions for this same model system. The legend is the same as in Figure 7.

an increase in the friction is observed. With a further increase in density, more molecules are crowded into those peripheral positions, and yet we find that the rotational diffusion constant increases somewhat, although it still remains smaller than the corresponding low-density result. What should we make of this behavior? It is possible that the aforementioned difficulty in modeling the correlation function oscillations at $\rho^* = 1.00$ is skewing the results at that point and leading us to underestimate that particular diffusion constant. On the other hand, if peripheral molecules must move out of the way as toluene rotates, then at the critical density a "critical slowing down" may be retarding the response of the solvent molecules to the relatively ponderous motion of the toluene and enhancing the friction.[2,11] Studies of similar systems will be required to elucidate this point further.

Finally, we have estimated the contribution of electrostatic effects in this system by performing a calculation identical to the one described above at $\rho^* = 1.00$ *except* that the partial charges on the atoms of toluene have been set to zero. The resulting molecule now has zero electrostatic moments. Results obtained from this calculation are shown in Figure 8 and in the rightmost column of Table 1. Most remarkably, in this case we find no real differences among the calculated rotational diffusion constants for motion about the orthogonal principal axes. This result is not necessarily surprising, though. The principal effect of including the partial charges is creating a strong preference for CO_2 to be found in the binding sites above and below the ring plane. In the absence of those charges, the solvent molecules arrange themselves around the toluene molecule more uniformly, causing any motion of the toluene to be uniformly retarded. It is clear that eliminating dipole−quadrupole electrostatic interactions alters the local ordering of the solvent, a result that also can be seen in the radial distribution function appropriate to this case (the thin line shown in Figure 5). One finds there a notable narrowing of the first-solvation-shell peak in comparison with the one determined using the full potential energy function and a loss of the peak shoulder corresponding to the previously preferred binding sites.

These final model calculations also are interesting in that they yield diffusion constants and friction coefficients for rotation

in the plane of the ring and for end-over-end tumbling that are essentially identical with those obtained when the full potential function is used. This result suggests that the local solvent structure (and in particular the local structure near the methyl group, since the same effect is not seen for rotation about the dipole axis) in the near-critical regime indeed is being significantly influenced by the appearance of long-range structural correlations in the solvent. The next step in this study would be to map more completely the density range over which this coincidence is found and to determine its dependence on the magnitude of the solvent's quadrupole moment.

V. Concluding Remarks

In this study we have investigated the rotational dynamics of a small, weakly polar solute in a nondipolar solvent characterized by a quadrupole moment that is large, particularly when viewed relative to the size of the solvent molecule. As anticipated, we find that the rotation of the toluene molecule is notably anisotropic, that, in general, the angular velocity about the axis perpendicular to the plane of the molecule relaxes on a time scale that is longer than that for the relaxation of the other two rotational degrees of freedom. Our results also hint, though, that the appearance of long-range spatial correlations in the near-critical regime may alter the details of the general tendency for the angular velocity relaxation to become faster as the solution density increases. Furthermore, we have provided an example in which "turning off" the electrostatic interactions between the solute and the solvent produces a dramatic change in the relaxation dynamics. It is worth emphasizing that we have done more than just eliminate the dipole−quadrupole interaction in our system—we have eliminated solute−solvent electrostatic forces entirely (although not those acting between solvent molecules). In future work we anticipate examining systems such as benzene-CO_2 (with and without partial charges on the carbon and hydrogen atoms of benzene) in which we can examine selectively the loss of the quadrupole−quadrupole interactions.

One of our goals when beginning this project was to evaluate the suitability of the toluene-CO_2 system as a target for experiments that probe inertial rotational dynamics. Information about free (or nearly free) rotation in such systems may be extracted from the parabolic time dependence of the orientational correlation functions $C_l(t)$ at short times. Even at the highest density considered, $C_l(t)$ is essentially parabolic and thus deviates from a simple exponential decay on a time scale of about a quarter of a picosecond, which is well within the temporal resolution of modern instrumentation.[52] Thus, we conclude that toluene may indeed be a useful solute for studies of rotational relaxation in SCFs. In fact, there are a host of small, substituted benzenes that also ought to be appropriate targets for such investigations, differing only in the nature of the specific interactions attributable to the substituents (e.g., −OH, $-NH_2$) and in the overall dipole moment of the molecule. The significance of these interactions in a nondipolar solvent is still uncertain, but we expect short-range dipole−quadrupole and quadrupole−quadrupole forces again to make an important contribution to the dynamical properties of these systems.

Acknowledgment. We are grateful to M. Khajehpour and J. Kauffman for providing the results of their recent work on quadrupolar fluids and for useful conversations regarding the present work. It is also our great pleasure to dedicate this paper to Bill Miller on the occasion of his 60th birthday.

References and Notes

(1) Biswas, R.; Lewis, J. E.; Maroncelli, M. *Chem. Phys. Lett.* **1999**, *310*, 485.
(2) Heitz, M. P.; Maroncelli, M. *J. Phys. Chem. A* **1997**, *101*, 5852.
(3) Song, W.; Biswas, R.; Maroncelli, M. *J. Phys. Chem. A* **2000**, *104*, 6924.
(4) Egorov, S. A. *J. Chem. Phys.* **2000**, *113*, 1950.
(5) Egorov, S. A. *J. Chem. Phys.* **2000**, *112*, 7138.
(6) Egorov, S. A.; Yethiraj, A.; Skinner, J. L. *Chem. Phys. Lett.* **2000**, *317*, 558.
(7) Adams, J. E. *J. Phys. Chem. B* **1998**, *102*, 7455.
(8) Goodyear, G.; Maddox, M. W.; Tucker, S. C. *J. Chem. Phys.* **2000**, *112*, 10327.
(9) Goodyear, G.; Maddox, M. W.; Tucker, S. C. *J. Phys. Chem. B* **2000**, *104*, 6258.
(10) Goodyear, G.; Maddox, M. W.; Tucker, S. C. *J. Phys. Chem. B* **2000**, *104*, 6240.
(11) Maddox, M. W.; Goodyear, G.; Tucker, S. C. *J. Phys. Chem. B* **2000**, *104*, 6266.
(12) Maddox, M. W.; Goodyear, G.; Tucker, S. C. *J. Phys. Chem. B* **2000**, *104*, 6248.
(13) Tucker, S. C.; Maddox, M. W. *J. Phys. Chem. B* **1998**, *102*, 2437.
(14) Jang, J.; Stratt, R. M. *J. Chem. Phys.* **2000**, *112*, 7538.
(15) Jang, J.; Stratt, R. M. *J. Chem. Phys.* **2000**, *112*, 7524.
(16) Reynolds, L.; Gardecki, J. A.; Frankland, S. J. V.; Horng, M. L.; Maroncelli, M. *J. Phys. Chem.* **1996**, *100*, 10337.
(17) Nee, T. W.; Zwanzig, R. *J. Chem. Phys.* **1970**, *52*, 6353.
(18) Berne, B. J.; Harp, G. D. In *Advances in Chemical Physics*; Prigogine, I., Rice, S. A., Eds.; Wiley: New York, 1970; Vol. 17, pp 63−227.
(19) Bruehl, M.; Hynes, J. T. *J. Phys. Chem.* **1992**, *96*, 4068.
(20) Mori, H. *Prog. Theor. Phys. (Jpn.)* **1965**, *33*, 423.
(21) Bursulaya, B. D.; Zichi, D. A.; Kim, H. J. *J. Phys. Chem.* **1996**, *100*, 1392.
(22) Kumar, P. V.; Maroncelli, M. *J. Chem. Phys.* **2000**, *112*, 5370.
(23) Papazyan, A.; Maroncelli, M. *J. Chem. Phys.* **1995**, *102*, 2888.
(24) Kurnikova, M. G.; Waldeck, D. H.; Coalson, R. D. *J. Chem. Phys.* **1996**, *105*, 628.
(25) Kurnikova, M. G.; Balabai, N.; Waldeck, D. H.; Coalson, R. D. *J. Am. Chem. Soc.* **1998**, *120*, 6121.
(26) Hartman, R. S.; Alavi, D. S.; Waldeck, D. H. *J. Phys. Chem.* **1991**, *95*, 7872.
(27) Balabai, N.; Waldeck, D. H. *J. Phys. Chem. B* **1997**, *101*, 2339.
(28) Spears, K. G.; Steinmetz, K. M. *J. Phys. Chem.* **1985**, *89*, 3623.
(29) Nelson, R. D.; Lide, D. R.; Maryott, A. A. *Natl. Stand. Ref. Data Serv., Natl. Bur. Stand. U.S.* **1967**, *10*, 1.
(30) Jorgensen, W. L.; Laird, E. R.; Nguyen, T. B.; Tirado-Rives, J. *J. Comput. Chem.* **1993**, *14*, 206.
(31) Buckingham, A. D.; Disch, R. L. *Proc. R. Soc. A.* **1963**, *273*, 275.
(32) Mataga, N.; Kubota, T. *Molecular Interactions and Electronic Spectra*; Marcel Dekker: New York, 1970.
(33) Khajehpour, M.; Kauffman, J. F. *J. Phys. Chem. A* **2000**, *104*, 9512.
(34) Myers, A. B.; Pereira, M. A.; Holt, P. L.; Hochstrasser, R. M. *J. Chem. Phys.* **1987**, *86*, 5146.
(35) Debye, P. *Polar Molecules*; Dover: New York, 1945.
(36) Adams, J. E. *J. Phys. Chem. B*, manuscript in preparation.
(37) Okazaki, S.; Matsumoto, M.; Okada, I. *J. Chem. Phys.* **1995**, *103*, 8594.
(38) Versmold, H. *Mol. Phys.* **1981**, *43*, 383.
(39) Böhm, H. J.; Meissner, C.; Ahlrichs, R. *Mol. Phys.* **1984**, *53*, 651.
(40) Singer, K.; Taylor, A. J.; Singer, J. V. L. *Mol. Phys.* **1977**, *33*, 1957.
(41) Singer, K.; Singer, J. V. L.; Taylor, A. J. *Mol. Phys.* **1979**, *37*, 1239.
(42) Harris, J. G.; Yung, K. H. *J. Phys. Chem.* **1995**, *99*, 12021.
(43) Murthy, C. S.; O'Shea, S. F.; McDonald, I. R. *Mol. Phys.* **1983**, *50*, 531.
(44) Jorgensen, W. L.; Tirado-Rives, J. *J. Am. Chem. Soc.* **1988**, *110*, 1657.
(45) Jorgensen, W. L.; Briggs, J. M.; Contreras, L. *J. Phys. Chem.* **1990**, *94*, 1683.
(46) Refson, K. Moldy; 2.15 ed., 1999.
(47) Refson, K. *Physica* **1985**, *131B*, 256.
(48) Allen, M. P.; Tildesley, D. J. *Computer Simulation of Liquids*; Oxford University Press: Oxford, U.K., 1992.
(49) Perng, B.-C.; Ladanyi, B. M. *J. Chem. Phys.* **1999**, *110*, 6389.
(50) Newitt, D. M.; Pai, M. U.; Kuloor, N. R.; Huggill, J. A. W. In *Thermodynamic Functions of Gases*; Din, F., Ed.; Butterworth: London, 1956; Vol. 123.
(51) Nowak, R.; Menapace, J. A.; Bernstein, E. R. *J. Chem. Phys.* **1988**, *89*, 1309.
(52) Baskin, J. S.; Chachisvilis, M.; Gupta, M.; Zewail, A. H. *J. Phys. Chem. A* **1998**, *102*, 4158.